U.S. CLIVAR VARIATIONS

Summer 2011, Vol. 9, No. 2

Atlantic Basin Research Challenges

by Michael Patterson, Director

This issue of Variations presents four articles highlighting modeling research presented at the CLIVAR-sponsored workshop on Coupled Ocean-Atmosphere-Land Processes in the Atlantic held in Miami, March 23-25, 2011. The workshop reviewed model biases in simulating the Atlantic (notably ocean circulation, sea surface temperatures, surface winds, clouds, and precipitation) and identified hypotheses on mechanisms responsible for the biases (see summary article on back page).

Kirtman et al. summarizes results of experiments using increased ocean model resolution to assesses the impact of resolved ocean fronts and eddies on the simulated mean large-scale climate. Brian Medeiros presents a comparison of simulated surface and atmospheric state of the eastern tropical Atlantic and Pacific stratocumulus regions, identifying differences in modeled characteristics of the two regions. Christina Patricola et al. investigate contributions of biases in westerly trade winds as well as Amazonian and tropical African precipitation to warm summer SST biases in the eastern equatorial Atlantic. Sang-Ki Lee et al. exam-

Continued on Page Two

IN THIS ISSUE

Impact of Ocean Model Resolution on CCSM Climate Simulations

Ben P. Kirtman[1], Cecilia Bitz[2], Frank Bryan[3], William Collins[4], John Dennis[3], Nathan Hearn[3], James L. Kinter[5] III, Richard Loft[3], Clement Rousset[1], Leo Siqueira[1], Cristiana Stan[5], Robert Tomas[3], and Mariana Vertenstein[3]

[1]University of Miami, Miami, Florida
[2]University of Washington, Seattle, Washington
[3]National Center for Atmospheric Research, Boulder, Colorado
[4]University of California, Berkeley, California
[5]Center for Ocean-Land-Atmosphere Studies, Calverton, Maryland

There is a growing demand for environmental predictions that include a broader range of space and time scales and that include a more complete representation of physical processes. Meeting this demand necessitates a unified approach that will challenge the traditional boundaries between weather and climate science, and will require a more integrated approach to the underlying Earth system science and the supporting computational science. One of the consequences of this unified or seamless approach is the need to explore much higher spatial resolution in weather and climate models. Increased model resolution has the potential to better resolve relevant features, and, more importantly, to accurately represent the interactions and feedbacks among the various physical and dynamical processes (Randall et al. 2003; Hurrell et al. 2009; Shukla et al. 2008; Brunet et al. 2010). It is also recognized that interactions across time and space scales are fundamental to the climate system itself. The large-scale climate, for instance, determines the environment for microscale (order 1 km) and mesoscale (order 10 km) variability which then feedback onto the large-scale climate. In the simplest terms, the statistics of microscale and mesoscale variability significantly impact the simulation of climate. In typical climate models at, say, 200 km horizontal resolution[1], these variations occur on unresolved scales, and the microscale and mesoscale processes are parameterized in terms of the resolved variables.

Several recent studies have focused on the importance of atmospheric model resolution in the simulation of climate (May and Roeckner 2001; Brankovic and Gregory 2001; Pope and Stratton 2002; Kobayashi and Sugi 2004; Hack et al. 2006; Navarra et al. 2008; Gent et al. 2009; Kinter et al. 2011). The reported results range from little or no change in the mean and variable climate (i.e., Hack et al. 2006) to significant differences in the cycle of El Niño and theSouthern Oscillation (ENSO; Navarra et al. 2008) and in sea surface temperature (SST) biases in the upwelling regions (i.e., Gent et al. 2009 – hereafter G09).

McClean et al. (2010) and Bryan et al. (2010) were the first to examine the question of the resolution dependence of simulations with CCSM (Community Climate System Model) that incorporated an eddy-resolving ocean component . In particular, McClean et al. (2010) used the same version of the CCSM component models as used in this study and G09, but with

[1]*Throughout this paper, model "resolution" refers to the spacing of model grid elements.*

Continued from Page One

ine the multi-decadal variability of the Atlantic Meridional Overturning Circulation (AMOC) and associated meridional ocean heat transport in the 20th Century.

Atlantic meridional heat transport was a focus of the 2011 US AMOC annual science meeting, held jointly with the UK Rapid Climate Change Programme in Bristol, UK, 12-15 July. Understanding Atlantic variability on a range of time scales was explored, with a main focus of the role of the AMOC. Presentation abstracts are available at http://www.noc.soton.ac.uk/rapid/ic2011/. Aditionally, the recently released Special Issue of *Deep-Sea Research II* entitled Climate and the Atlantic Overturning Meridional Circulation presents a series of papers on observing and monitoring the characteristics of AMOC, methods for tracking overturning transports, predictability and prediction, and the potential for abrupt climate change (see http://www.elsevier.com/wps/find/journaldescription.cws_home/116/description).

Finally, I wish to take this opportunity to announce my acceptance of the permanent position of the U.S. CLIVAR Office Director, effective May 31, 2011. I look forward to engaging the US climate research community and the US climate research funding agencies in the months and years ahead to advance climate science planning and implementation in the US and to foster fruitful international collaborations.

Variations

U.S. CLIVAR Office
1717 Pennsylvania Ave., NW
Suite 250, Washington, DC 20006
usco@usclivar.org

Staff: **Michael Patterson**, *Editor*
Cathy Stephens, *Assistant Editor and Staff Writer*

horizontal atmospheric model resolution of approximately 0.25º coupled to the 0.1º ocean component. The coupled model was run for 20 years, and produced simulated SST that is too cold in the sub-polar and mid-latitude Northern Hemisphere, but more realistic Aghulas eddy pathways compared to ocean-only simulations at comparable resolution. Bryan et al. (2010) examined the McClean et al. (2010) simulation as well as two additional experiments separately probing the ocean and atmospheric model resolution. As in McClean et al. (2010), the Bryan et al. (2010) simulations were run for approximately 20 years. Bryan et al. (2010) focused primarily on the coupling between the lower atmosphere and the SST, and found a more realistic pattern of positive correlation between high-pass filtered surface wind speed and SST when t he ocean component model is eddy-resolving. Both of these earlier studies are viewed as predecessors for the present work. The fundamental difference is that the focus of this work is on climate variability, which requires simulations of much longer duration than 20 years. Additional details and results from the work presented here can be found in Kirtman et al. (2011).

2. Model Configure and Experimental Design

a. CCSM3.5

The model used for this study is the NCAR Community Climate System Model version 3.5 (CCSM3.5) (Neale et al. 2008; G09). The atmospheric component model, the Community Atmospheric Model (CAM), is based on a finite volume discretization rather than the spectral discretization of the governing equations used in earlier versions of CAM, and has extensive changes in the parameterization of sub-grid-scale processes that have resulted in a significant improvement in the simulation of tropical variability relative to CCSM3.0 (Neale et al. 2008). Changes in the other component models, while less extensive, have also contributed to a reduction in systematic biases (Jochum et al. 2008; G09).

b. Increasing the Ocean Model Resolution

Two experiments are reported here. The first experiment (i.e., control, referred to as LRC) is a 155-year present-day climate simulation of the 0.5º atmosphere (zonal resolution 0.625º, meridional resolution 0.5º) coupled to ocean and sea-ice components with zonal resolution of 1.2º and meridional resolution varying from 0.27º at the equator to 0.54º in the mid-latitudes on a dipole grid (Murray, 1996) with 60 vertical levels. This control experiment is identical to the "high-resolution" experiment in G09 in terms of the model configuration, but differs in its initial state and climate forcing. The G09 experiment was a transient climate simulation initialized with a state extracted at year 1980 from a 20th century integration of the model at coarser resolution. The initial condition for our experiments was taken from the end of a previously completed present day control simulation carried out with an earlier version of CCSM, so that the ocean state is fully "spun-up" and the initialization shock ought to be minimized; however, as will be shown, some climate drift remains. The second simulation uses the same atmospheric model coupled to 0.1º ocean and sea-ice component models and will be referred to as HRC06. The ocean model configuration in this case is identical to the coupled climate simulation of McClean et al. (2011). In addition to the change in horizontal resolution from the control experiment, there are commensurate changes in the parameterization of horizontal sub-grid scale dissipation, and use of a different, 42-level vertical grid.

3. Results

One of the key motivating factors for this study is to assess how resolved ocean fronts and eddies impact the simulated mean large-scale climate. Specifically, Fig. 1a shows the North Atlantic SST climatology from HRC06 (shaded) and LRC superimposed (black contours). Fig. 1b is in the same format, except the figure shows the climatological rainfall. In terms of the surface temperature, HRC06 produces much sharper

[2] In common parlance, eddy-resolving models have horizontal resolution of less than 1/6º, in contrast to coarse-resolution models with 1º or greater grid spacing or eddy-permitting ocean models whose resolution lies between 1/6º and 1º.

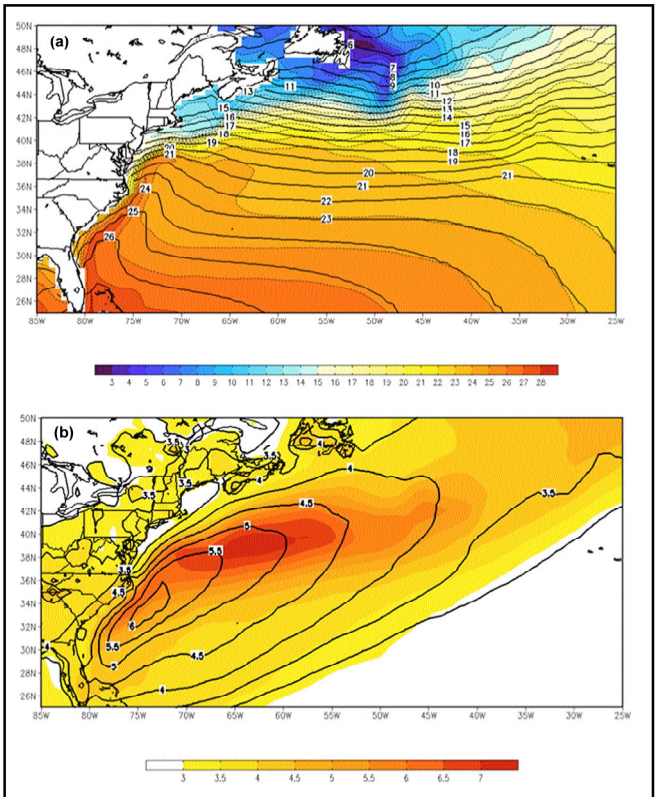

Figure 1. (a) Annual mean SST in the North Atlantic for HRC06 (shaded) and for LRC (contour) in degrees Celsius. (b) Annual mean surface current speeds in cm sec-1 for HRC (shaded) and LRC (contour).

gradients than LRC along the coast of North America and in the Gulf Stream separation region. Figure 1b indicates significant structural changes in the simulated rainfall associated with ocean model resolution. For example, the axis of maximum rainfall in HRC06 follows the maximum SST gradient so that the rainfall hugs the US coast and extends out into the open Atlantic as part of the Gulf Stream extension. The LRC simulation captures some aspects of the rainfall maximum along the US coast, but perhaps as expected, fails to capture the east-west oriented maximum along the Gulf Stream extension.

With respect to how higher ocean model resolution impacts the seasonal-to-interannual variability, we concentrate on the monthly mean SST anomalies (SSTA). Figure 2a, for example, shows the ratio of the SSTA monthly standard deviation for HRC06 compared to LRC. The standard deviation is calculated on the atmospheric model grid. The SST variability applied to the atmosphere is clearly enhanced in HRC06 throughout most of the mid-latitudes and the subtropics. The core regions of substantially enhanced variance include the Northern Hemisphere western boundary current zones and the Southern Ocean from the Atlantic coast of South America extending through to the Pacific side of the Australian continent.

In contrast to the extra-tropics, throughout most of the tropical ocean there is a reduction of variance in the eddy-resolving simulation (HRC06). Figure 2b indicates that there is a robust reduction of variability in the tropical Pacific. There are two aspects to this reduction of variance that are of particular interest. First, there is a nearly uniform reduction along the equator of 0.2ºC in the ENSO-related standard deviation. We hypothesize that the reduction of ENSO variance is an indirect effect of the ubiquitous ocean surface warming (see Fig. 2b) and modest increases in ocean stratification in the Pacific that ultimately lead to a small reduction in the ENSO variance (similar to the CCSM response to doubled CO2 levels – see Collins et al. 2010). This reduced ENSO variability leads to reduced variance in the tropical Indian Ocean and the north tropical Atlantic via well-known teleconnections.

The second aspect of interest in the reduction of variance in Fig. 2b appears as a subtle feature; namely, the standard deviation in HRC06 in the western Pacific between 140ºE and 160ºE has a pronounced plateau compared to LRC. This is a distinctly positive aspect of the HRC06 simulation compared to the observed variance shown in Fig. 2b. For instance, most current coupled models produce ENSO variance that extends too far into the western Pacific leading to ENSO teleconnections that have the wrong sign in the western Pacific. Kirtman and Vecchi (2010), Wu and Kirtman (2007) and Wu et al. (2007) argue heuristically that the excessive variance and teleconnection errors are due to "excessive coupling" between the atmosphere and the ocean. We hypothesize that the enhanced ocean resolution in HRC06 has the effect of adding relatively high frequency noise (see Fig. 2c) to the coupled system and destructively interfering with the excessive coupling.

Figure 2c shows the high-pass filtered SSTA standard deviation along the equator for 10 years[3] of daily data from LRC and HRC06 respectively. The high-pass filtered standard deviation is larger for HRC06 compared to LRC indicating that the eddies enhance the variance but primarily at sub-monthly time scales.

In keeping with the objective to examine how resolved ocean fronts and eddies impact the large-scale climate, the results obtained suggest some notable climatic impacts. For example: (i)The SST front associated with the Gulf Stream is better resolved in the high-resolution simulation. This leads to large structural changes in the mean rainfall. Similar changes in the currents are seen in the vicinity of the Kuroshio, but the increased ocean resolution is apparently not as important for maintaining the SST gradient, as the temperature and rainfall differences are small compared to those near the Gulf Stream. (ii)As expected, the variability of monthly mean SSTA increases with increasing ocean resolution throughout the extra-tropics. This increase is most notable in the western boundary current regions and the Southern Ocean. Contrary to expectation, ENSO variability decreases and some of the associated tropical SSTA teleconnections are weaker. (iii)The structure of the SSTA variability along the equator in the western Pacific also is quite different in HRC06 and LRC. There is a distinct plateau in the variability in HRC06 that is consistent with reduced coupling and ENSO

[3]Only 10 years of daily data was available for this calculation.

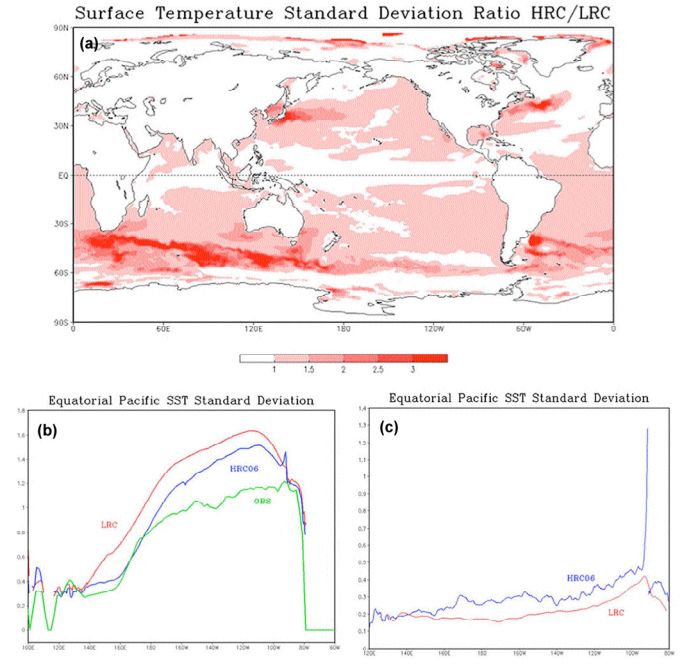

Figure 2.(a) SSTA monthly mean standard deviation ratio (HRC06/LRC) - dimensionless. Values greater than 1.0 indicate more variance in HRC06. (b) SSTA monthly mean standard deviation near the equator (1S-1N) in the Pacific for LRC (red) and HRC06 (blue) in degrees Celsius. Observational estimates are given in green. (c) SSTA high pass filtered SSTA standard deviation near the equator (1S-1N) in the Pacific for LRC (red) and HRC06 (blue).

events that do not extend as far to the west as in the case of LRC.

Acknowledgements:

We acknowledge the support of the National Science Foundation (J. Kinter and C Stan through AGS 0830068 and OCI 0749290; B. Kirtman through OCI 0749165, AGS 0754341 and AGS 0850897; C. Bitz through ARC 0938204; F. Bryan, J. Dennis, N. Hearn, R. Loft, R. Tomas and M. Vertenstein through its support of NCAR). B. Kirtman also acknowledges support from NOAA NA08OAR3420889. Computing resources were provided by the National Institute of Computational Sciences at the University of Tennessee through an award made by the TeraGrid Resource Allocations Committee.

References

Brankovic C. and Gregory D., 2001: Impact of horizontal resolution on seasonal integrations. Clim. Dyn., 18:123–143. doi:10.1007/s003820100165.

Brunet, G., and Coauthors, 2010: Collaboration of the Weather and Climate Communities to Advance Subseasonal-to-Seasonal Prediction. Bull. Amer. Meteor. Soc., 91, 1397–1406.

Bryan, F. O., R. Tomas, J. M. Dennis, D. B. Chelton, N. G. Loeb, J. L. McClean, 2010: Frontal scale air–sea interaction in high-resolution coupled climate models. J. Climate, 23, 6277–6291. doi: 10.1175/2010JCLI3665.1

Collins, M., and co-authors, 2010: The impact of global warming on the tropical Pacific Ocean and El Nino. Nature Geoscience, 3, 391-397.

Gent, P.R., S.G. Yeager, R.B. Neale, S. Levis, and D.A. Bailey, 2009: Improvements in a half degree atmosphere/land version of the CCSM. Clim. Dynamics, 34, 819-833.

Hack JJ, Caron JM, Danabasoglu G, Oleson KW, Bitz C, Truesdale JE (2006) CCSM–CAM3 climate simulation sensitivity to changes in horizontal reslution. J. Climate, 19, 2267–2289, doi: 10.1175/JCLI3764.1.

Hurrell, J., G. A. Meehl, D. Bader, T. L. Delworth, B. Kirtman, B. Wielicki, 2009: A unified modeling approach to climate system prediction. Bull. Amer. Meteor. Soc., 90, 1819–1832.

Jochum M, Danabasoglu G, Holland MM, Kwon YO, Large WG (2008) Ocean viscosity and climate. J. Geophys. Res., 113, doi:10.1029/2007JC004515.

Kinter III, J. L., B. Cash, D. Achuthavarier, J. Adams, E. Altshuler, P. Dirmeyer, B. Doty, B. Huang, L. Marx, J. Manganello, C. Stan, T. Wakefield, E. Jin, T. Palmer, M. Hamrud, T. Jung, M. Miller, P. Towers, N. Wedi, M. Satoh, H. Tomita, C. Kodama, T. Nasuno, K. Oouchi, Y. Yamada, H. Taniguchi, P. Andrews, T. Baer, M. Ezell, C. Halloy, D. John, B. Loftis, R. Mohr, and K. Wong, 2011: Revolutionizing climate modeling – Project Athena: A multi-institutional, international collaboration. Bull. Amer. Meteor. Soc. (submitted).

Kirtman, B.P., and G. Vecchi, 2010: Why Climate Modelers Should Worry About the Weather. WMO Monograph: The Global Monsoon System: Research and Forecast, 2nd Ed.

Kirtman, B. P., C. Bitz, F. Bryan, W. Collins, J. Dennis, N. Hern, J. L. Kinter III, R. Loft, C. Rousset, L. Siqueira, C. Stan, R. Tomas, and M. Vertenstein, 2011: Impact of ocean model resolution on CCSM climate simulations. Clim. Dyn. (submitted).

Kobayashi C. and Sugi, M., 2004: Impact of horizontal resolution on the simulation of the Asian summer monsoon and tropical cyclones in the JMA global model. Clim. Dyn., 23, 165–176. doi:10.1007/s00382-004-0427-8.

May W, and Roeckner, E., 2001: A time-slice experiment with the ECHAM4 AGCM at high resolution: the impact of horizontal resolution on annual mean climate change. Clim. Dyn., 17, 407–420, doi:10.1007/s003820000112.

McClean, J.L., D.C. Bader, F.O. Bryan, M.E. Maltrud, J.M. Dennis, A.A. Mirin, P.W. Jones, M. Vertenstein, D.P. Ivanova, Y.-Y. Kim, J.S. Boyle, R.L. Jacob, N. Norton, A. Craig, and P.H. Worley, 2010:A prototype two decade fully coupled fine resolution CCSM simulation. J. Climate (submitted).

Murray, R., 1996: Explicit generation of orthogonal grids for ocean models. J. Comp. Phys., 126, 251-273.

Navarra A et al., 2008: Atmospheric horizontal resolution affects tropical climate variability in coupled models. J. Climate, 21,730– 750, doi:10.1175/2007JCLI1406.1.

Neale, R.B., J.H. Richter, and M. Jochum, 2008: The impact of convection on ENSO: from a delayed oscillator to a series of events. J. Climate, 21, 5904-5924.

Pope V, and Stratton R, 2002: The processes governing horizontal resolution sensitivity in a climate model. Clim. Dyn., 19, 211–236. doi:10.1007/s00382-001-0222-8.

Randall, D. A., M. Khairoutdinov, A. Arakawa , and W. Grabowski, 2003: Breaking the cloud-parameterization deadlock. Bull. Amer. Meteor. Soc., 84, 1547–1564.

Shukla, J., R. Hagedorn, M. Miller, T. N. Palmer, B. Hoskins, J. Kinter, J. Marotzke, J. Slingo, 2009: Strategies: Revolution in climate prediction is both necessary and possible: A declaration at the World Modelling Summit for Climate Prediction. Bull. Amer. Meteor. Soc., 90, 175–178.

Wu, R., and B. P. Kirtman, 2007: Regimes of local air-sea interactions and implications for performance of forced simulations. Climate Dynamics, 29, 393-410.

Wu, R., B. P. Kirtman, and K. Pegion, 2007: Surface latent heat flux and its relationship with sea surface temperature in the National Centers for Environmental Prediction Climate Forecast System simulations and retrospective forecasts. Geophys. Res. Lett., 34, L17712, doi:10.1029/2007GL030751.

Comparing the Southern Hemisphere Stratocumulus Decks in the Community Atmosphere Model

Brian Medeiros,
National Center for Atmospheric Research, Boulder, Colorado

Viewed from space, the subtropical stratocumulus decks appear as bright sheets of cloud anchored to the west coasts of continents sweeping toward the deeper tropics. Closer inspection shows that these large climatological features consist of thin clouds lying atop a well-mixed atmospheric boundary layer just a few hundred meters above the surface. These characteristics – large areal coverage, low altitude, and high reflectivity – make the subtropical stratocumulus decks conspicuous in the global energy budget (e.g., Ramanathan et al., 1989). Because of their connection to the energy budget, stratocumulus decks have been the target of many observational campaigns; 20th Century investigations focused mainly on stratocumulus in the northern hemisphere. The last decade witnessed increased interest in, and relatively sustained observations of the southeast Pacific stratocumulus deck (n.b., EPIC (Bretherton et al., 2004) and VOCALS-REx (Wood et al., 2011)).

Compared to the southeast Pacific, the southeast Atlantic stratocumulus deck has remained obscure. While its existence has long been recognized (e.g., Schubert et al., 1979), including its large extent and seasonality (Hanson, 1991; Klein and Hartmann, 1993), there are limited in situ observations, few satellite-based studies, and a handful of modeling studies of this feature. This apparent lack of interest is surprising because the tropical Atlantic, especially near the coast of southwestern Africa, has been noted for large, persistent sea-surface temperature biases in climate models. Cloud-SST feedback has been a favored explanation for the biases (Wahl et al., 2011), so understanding the characteristics of the cloud deck and representing these clouds in climate models should be a priority for the climate modeling community.

The latest version of the NCAR climate model, the Community Earth System Model (CESM), contains improvements across the component models. Among these are major changes in the parameterized physical processes in the Community Atmosphere Model, Version 5 (CAM5), many of which directly affect the representation of clouds. Despite the changes, coupled simulations continue to exhibit temperature biases near eastern boundary currents, particularly in the southeast Atlantic.

Inspired by recent evaluations of southeast Pacific stratocumulus in models (Wyant et al., 2010; Hannay et al., 2009), we revisited the southeast Pacific with two versions of CAM recently released: CAM4[1] which closely resembles previous versions, and CAM5[2] which incorporates many changes introduced with the CESM. The results show that the updated physics produce more realistic stratocumulus, but some important deviations from observations remain that could impact climate simulations (Medeiros et al., 2011). As an extension of that work, we performed simulations with CAM5, described below, of the southeast Atlantic stratocumulus deck. Because observations are more limited for the southeast Atlantic, a validation of the model is difficult, but it is interesting to compare and contrast the two major southern hemisphere stratocumulus decks as represented by CAM5.

To focus on the parameterized physics associated with the subtropical stratocumulus decks, we use a short-term forecast framework that mimics the forecast/analysis cycle of numerical weather prediction (Phillips et al., 2004; Boyle and Klein, 2010). The principle is simple: perform short forecasts with a climate model by starting from an observed atmospheric state. The benefit is that the large-scale circulation adjusts away from the realistic conditions slowly, while the fast processes (i.e., parameterized physics) act quickly, so forecast errors are tied to parameterization errors. This allows a close inspection of parameterized processes within a realistic large-scale setting, but precludes investigating the model's climatological behavior (e.g., seasonality or interannual variability). Here we apply this framework to produce 5-day forecasts from CAM5 with 3-hourly output saved for both the southeast Pacific and the southeast Atlantic. The forecasts cover October 2006, as October is climatologically the month during which the stratocumulus decks reach their maximum spatial extent. A new forecast begins each day at midnight UTC, starting from the atmospheric state derived from ECMWF operational analyses (for details, see Medeiros et al., 2011).

Figure 1 summarizes the environmental conditions simulated for October 2006. The figure composites the forecasts by averaging all forecasts over days 2-5, which avoids any initialization artifacts that might occur in the first hours. Both regions are strongly influenced by subtropical anticyclones, with southerly and southeasterly winds blowing along the coast as the circulation rounds the eastern flank of the high pressure centers. These winds induce Ekman transport and coastal upwelling that help to keep the sea-surface cool, though in these forecasts surface temperature is set to the observed values. The streamlines cross isolines of sea-surface temperature traveling toward the trades, signaling low-level cold

[1] http://www.cesm.ucar.edu/models/ccsm4.0/cam/
[2] http://www.cesm.ucar.edu/models/cesm1.0/cam/

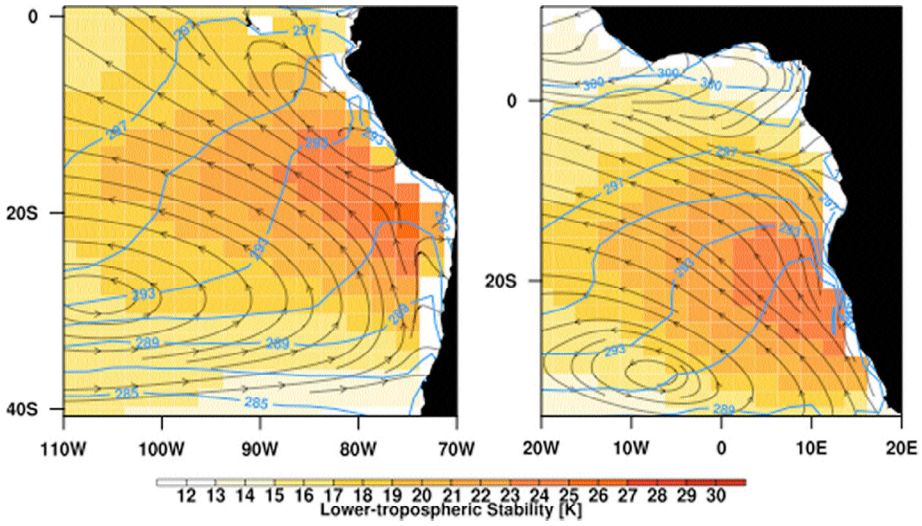

Figure 1. Streamlines at 850 hPa for CAM5 forecasts of the (left) southeast Pacific and (right) southeast Atlantic for October 2006. The color contours show average lower-tropospheric stability. Blue contour lines show the prescribed sea-surface temperature (K).

advection. Above the atmospheric boundary layer, large-scale sinking motion delivers warm, dry air to the lower troposphere. Where this warm, dry air meets the cool, moist boundary layer air the trade wind inversion is found. The inversion is sharp in the stratocumulus regions, occurring in less than 100 m (e.g., Fedorovich et al., 2004), and cloud amount is correlated with inversion strength on seasonal timescales (Klein and Hartmann, 1993). Simulating the inversion is a challenge for climate models because of their coarse vertical resolution; the CAM5 is typical of these models with 30 vertical levels, 8 of which are below 800 hPa. Even so, the model captures some semblance of the inversion. A crude proxy for the inversion strength is the so-called lower-tropospheric stability (the difference between the 700 hPa and surface potential temperatures), shown by the colored field in Figure 1.

The simulated cloud fraction and liquid water path are shown in Figure 2. Comparing Figures 1 and 2, the correspondence between lower-tropospheric stability and cloud amount is evident. In both regions, the maximum cloud cover is displaced downstream from the maximum stability. This displacement may be due local effects near the coast, but warrants further investigation. Compared to satellite observations of October 2006, the cloud distributions for both regions appear realistic, though less cloudy than some estimates. This low bias has been typical for climate models for many years. Related to this bias, in the southeast Pacific the cloud deck dissipates too close to the continent.

The large-scale conditions appear fairly similar for the two regions, and the cloud patterns are roughly commensurate with those conditions and resemble observations from the same time.

The vertical structure of the clouds, however, contains some subtle differences. An example is shown by Figure 3, which shows the composite forecast (averaging all forecasts provides an estimate of the monthly mean for each forecast time) of cloud fraction and cloud liquid water for a single grid point in each region. The southeast Pacific point shows the location nearest a moored buoy that has been the focus of substantial study (e.g., de Szoeke et al., 2010). Without a similar target for the southeast Atlantic, a point was chosen with a similar mean (vertically integrated) low-cloud fraction (printed in the figure). The figure illustrates two differences between the regions. First, the southeast Pacific has a larger diurnal cycle of cloud cover. Second, the cloud-base, and to a lesser extent cloud-top, is less well defined (i.e., gradients are less sharp) in the southeast Atlantic. While the figure shows averages for just two individual points, these characteristics appear to be robust within the stratocumulus decks.

Both stratocumulus regions show a clear diurnal cycle, with maximum cloud cover during night and early morning, consistent with observations. Capturing the correct diurnal behavior is crucial for climate simulations because these clouds impact the global energy balance through their shortwave effects. Underestimating the cloud frac-

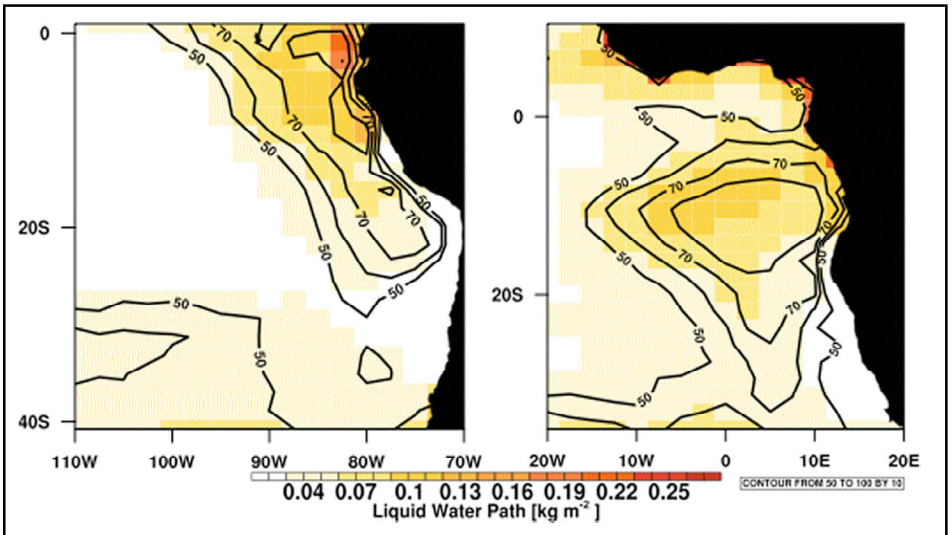

Figure 2. Average low-cloud fraction (contour lines, %) and liquid water path (color, kg m^2) simulated by CAM5 for October 2006.

tion during the daytime undercuts the climatic impact of the clouds, and could lead to positive cloud-sea surface temperature feedbacks. Medeiros et al. (2011) suggest that the daytime breakup of the southeast Pacific cloud deck is exaggerated by CAM5. As shortwave heating in the cloud layer compensates longwave cooling, the cloud layer and subcloud layer become decoupled, cutting off the cloud layer from its moisture source. Along with the decoupling, shallow cumulus convection rises through the cloud layer and entrains warm, dry air that enhances cloud evaporation. Such decoupling is common in the southeast Pacific, but the cloud dissipation in CAM5 is excessive, weakens the cloud radiative effect, and could lead to climate biases.

The southeast Atlantic clouds exhibit a smaller amplitude diurnal cycle than the southeast Pacific, and the difference is in the daytime minimum. The cloud-top appears lower for the Atlantic stratocumulus, which is consistent with satellite observations (Zuidema et al., 2009). Cloud-base also appears lower. The boundary layer depth is similar between the regions, though the lifting condensation level (LCL) is lower and more variable in the southeast Atlantic. The variability in LCL explains why the cloud-base level is not distinct in the region. The difference between the boundary layer depth and the LCL approximates the thickness of the cloud layer or (when the difference is small) decoupling. Using this diagnostic, decoupling is less frequent in the southeast Atlantic than southeast Pacific. Since the cloud layer breaks up more easily once decoupled, this difference between the regions probably accounts for the difference in daytime cloud fraction and might explain the difference in the size of the stratocumulus decks during this month. The less frequent decoupling in the Atlantic might imply some southeast Pacific biases are regionally specific.

This comparison of the southern hemisphere stratocumulus decks raises some interesting questions. First among these is: given the limited temporal scope of the forecasts, how do these stratocumulus decks vary on longer timescales, both in the model and in reality? That answer could help to address a second question: is the less frequent decoupling, and smaller diurnal cycle, in the southeast Atlantic a persistent difference? These issues can be examined in the model, but it is not clear if suitable observations exist to compare the regions. If these differences are typical, what is the cause, given the similarity in the large-scale environment? Are precipitation or aerosol processes important, or do regional influences (e.g., nearby topography) introduce idiosyncrasies to the subtropical stratocumulus decks? Answering such questions will require detailed in situ observations, comprehensive satellite data sets, and focused modeling studies, and the answers may provide new insight about the climatic relevance of stratocumulus decks.

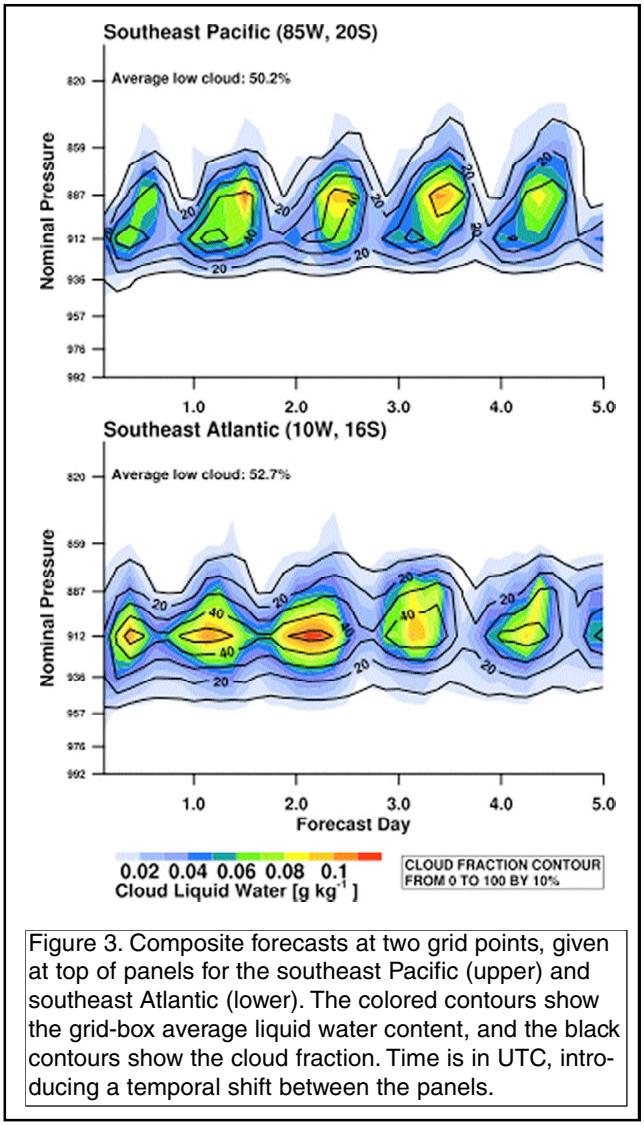

Figure 3. Composite forecasts at two grid points, given at top of panels for the southeast Pacific (upper) and southeast Atlantic (lower). The colored contours show the grid-box average liquid water content, and the black contours show the cloud fraction. Time is in UTC, introducing a temporal shift between the panels.

Acknowledgement

The author thanks ECMWF for providing the analysis data, and D. L. Williamson, J. E. Kay, and Y. Zhang for their thoughtful comments. This work was supported by the Office of Science (BER), U.S. Department of Energy, Cooperative Agreement DE-FC02-97ER62402. NCAR is sponsored by the National Science Foundation.

References

Boyle, J. and S. Klein, 2010: Impact of horizontal resolution on climate model forecasts of tropical precipitation and diabatic heating for the TWP-ICE period. J. Geophys. Res., 115 (D23), D23113, doi: 10.1029/2010JD014262.

Bretherton, C. S., et al., 2004: The EPIC 2001 stratocumulus study. Bull. Amer. Meteor. Soc., 85 (7), 967–977, doi:10.1175/BAMS-85-7-967.

de Szoeke, S. P., C. W. Fairall, D. E. Wolfe, L. Bariteau, and P. Zuidema, 2010: Surface flux observations on the southeastern tropical Pacific Ocean and attribution of SST errors in coupled ocean–atmosphere models. J. Climate, 23 (15), 4152–4174, doi:10.1175/2010JCLI3411.1.

Fedorovich, E., R. Rotunno, B. Stevens, and D. Lilly, (Eds.), 2004: Atmospheric turbulence and mesoscale meteorology: scientific research inspired by Doug Lilly. Cambridge University Press.

Hannay, C., D. L. Williamson, J. J. Hack, J. T. Kiehl, J. G. Olson, S. A. Klein, C. S. Bretherton, and M. Köhler, 2009: Evaluation of forecasted southeast Pacific stratocumulus in the NCAR, GFDL, and

ECMWF models. J. Climate, 22 (11), 2871–2889, doi:10.11752F2008JCLI2479.1.

Hanson, H. P., 1991: Marine stratocu - mulus climatologies. International Journal of Climatology, 11 (2), 147–164, doi:10.1002/joc.3370110204.

Klein, S. A. and D. L. Hartmann, 1993: The seasonal cycle of low stratiform clouds. J. Climate, 6, 1587–1606.

Medeiros, B., D. L. Williamson, C. Hannay, and J. G. Olson, 2011: Southeast Pacific stratocumulus in the Community Atmosphere Model (in preparation).

Phillips, T. J., et al., 2004: Evaluating parameterizations in general circulation models: Climate simulation meets weather prediction. Bull. Amer. Meteor. Soc., 85 (12), 1903–1915, doi:10.1175/BAMS-85-12-1903.

Ramanathan, V., B. R. Barkstrom, and E. F. Harrison, 1989: Climate and the Earth's radiation budget. Physics Today, 42 (5), 22–32, doi:10.1063/1.881167.

Schubert, W. H., J. S. Wakefield, E. J. Steiner, and S. K. Cox, 1979: Marine stra - tocumulus convection. Part I: Governing equations and horizontally homogeneous solutions. J. Atmos. Sci., 36, 1286–1307.

Wahl, S., M. Latif, W. Park, and N. Keenlyside, 2011: On the tropical Atlantic SST warm bias in the Kiel climate model. Climate Dynamics, 36, 891–906, doi:10.1007/s00382-009-0690-9.

Wood, R., et al., 2011: The VAMOS Ocean-Cloud-Atmosphere-Land Study Regional Experiment (VOCALS- REx): goals, platforms, and field operations. Atmos. Chem. Phys., 11 (2), 627–654, doi:10.5194/acp-11-627-2011.

Wyant, M. C., et al., 2010: The PreVOCA experiment: modeling the lower troposphere in the Southeast Pacific. Atmos. Chem. Phys., 10 (10), 4757–4774, doi:10.5194/acp-10-4757-2010.

Zuidema, P., D. Painemal, S. de Szoeke, and C. Fairall, 2009: Stratocumulus cloud-top height estimates and their climatic impli - cations. J. Climate, 22 (17), 4652–4666, doi:10.1175/2009JCLI2708.1.

Calendar of CLIVAR and CLIVAR-related meetings

Further details are available on the U.S. CLIVAR and International CLIVAR web sites: www.usclivar.org and www.clivar.org

CLIVAR Working Group on Seasonal to Interannual Prediction
12-14 September 2011
Trieste, Italy
Attendance: Invited
http://www.clivar.org/organization/wgsip/wgsip14/wgsip14.php

Land-Ocean Interactions in the Coastal Zone (LOICZ) Conference
12-15 September 2011
Yantai, China
Attendance: Open
http://www.loicz-osc2011.org/

ICES Annual Science Conference
19-23 September 2011
Gdansk, Poland
Attendance: Open
http://www.ices.dk/iceswork/asc/2011/index.asp

3rd Symposium on the Ocean in a High-CO2 World
24-27 September 2011
Monterey, California
Attendance: Open
http://www.highco2_iii.org/main.cfm?cid=2259&nid=14766

SAMOC4 Meeting
27-29 September 2011
Simons Town, South Africa
Attendance: Open
http://www.aoml.noaa.gov/phod/SAMOC

CLIVAR Working Group on Coupled Modeling
19-21 October 2011
Boulder, CO
Attendance: Invited
http://www.clivar.org/wgcm/wgcm-15/wgcm15.php

CLIVAR/CliC/SCAR Southern Ocean Panel Meeting
19-21 October 2011
Boulder, CO
Attendance: Invited
http://www.clivar.org/organization/southern/SOP7_meet.php

Interdisciplinary Climate Change Research Symposium
22-29 October 2011
Colorado Springs, CO
Attendance: Limited
http://disccrs.org/

WCRP Open Science Conference
24-28 October 2011
Denver, CO
Attendance: Open
http://www.wcrp-climate.org/conference2011/

International Conference on Energy and Meteorology
8-11 November 2011
Gold Coast, Australia
Attendance: Open
http://www.icem2011.org/

Earth Observation for Ocean-Atmosphere Interactions Science
29 November - 2 December 2011
Frascati, Italy
Attendance: Open
http://www.eo4oceanatmosphere.info/

AGU Fall Meeting
5-9 December 2011
San Francisco, CA
Attendance: Open
http://sites.agu.org/fallmeeting/

An Investigation of the Tropical Atlantic Bias Problem Using a High-Resolution Coupled Regional Climate Model

Christina M. Patricola[1], Ping Chang[2], R. Saravanan[1], Mingkui Li[3], and Jen-Shan Hsieh[1]

[1]Department of Atmospheric Sciences, Texas A&M University, College Station, Texas
[2]Department of Oceanography, Texas A&M University, College Station, Texas
[3]Ocean University of China, Qingdao, China

Coupled atmosphere-ocean general circulation models (AOGCMs) have long been plagued by biases in the tropical Atlantic. Observed SSTs in the eastern equatorial Atlantic cool by ~5°C from May to August as the Atlantic cold tongue forms, however, AOGCMs without flux correction fail to capture this (Davey et al. 2002; Breugem et al. 2006; Richter and Xie 2008). The cold tongue development is sensitive to the cross-equatorial southerly flow of the West African monsoon (Philander and Pacanowski 1981; Mitchell and Wallace 1992), and the monsoon is in turn influenced by regional SSTs (Lamb 1978; Ward 1998; Vizy and Cook 2002). Thus, the inability of coupled models to realistically represent the tropical Atlantic compounds the uncertainty of future climate change simulations.

The typical tropical Atlantic warm SST bias covers two regions – the eastern equatorial Atlantic (EEA) and southeastern tropical Atlantic (SETA) – and several distinct bias mechanisms have been proposed, including interactions between the two. Modeling studies suggest that an under-representation of low-level clouds and the associated excessive surface shortwave radiation (Huang et al. 2007; Wahl et al. 2011), an under-representation of coastal upwelling (Large and Danabasoglu 2006), and sensitivity to entrainment efficiency at the base of the ocean mixed layer (Hazeleger and Haarsma 2005) contribute to SST bias in the SETA. Xu et al. (2011) recently find that warm sub-surface temperature bias in the EEA can be advected south by sub-surface currents and upwelled along the Benguela coast, contributing to the warm SST bias in the coastal upwelling zone.

Several studies demonstrate that the EEA SST bias is connected to a springtime westerly equatorial trade wind bias (DeWitt 2005) that erroneously deepens the thermocline, inhibiting the summer cold tongue development (Chang et al. 2007; Richter and Xie 2008; Richter et al. 2011; Wahl et al. 2011). Uncoupled AGCM simulations with observed SSTs also simulate the trade wind bias, but relatively weakly, suggesting that it originates in atmospheric models and is amplified by the Bjerknes feedback (Bjerknes 1969) in coupled models. These studies link the trade wind bias to a zonal pressure gradient driven by deficient (excessive) rainfall over the Amazon (tropical Africa), although Chang et al. (2008) find the Amazon is the primary driver.

The formation of spurious oceanic barrier layers (BLs), which reduce entrainment and turbulent mixing of cold water at depth into the mixed layer, may also contribute to the warm EEA SST bias (Breugem et al. 2008). A southward bias of the intertropical convergence zone (ITZC) is common in atmospheric GCMs (Biasutti et al. 2006), and in coupled models it may initiate a positive ITCZ – BL – SST feedback, in which the freshwater flux of the displaced ITCZ reduces the ocean surface salinity, supporting BL formation and warmer SSTs, further anchoring the ITCZ. However, unrealistic BLs are not in all coupled simulations (Wahl et al. 2011; Richter et al. 2011), suggesting they may be a secondary error source (Balaguru et al. 2011).

Here we test the hypothesis that a springtime westerly trade wind bias, which is linked to deficient (excessive) Amazon (Congo basin) precipitation, contributes to the warm summer EEA SST bias by unrealistically deepening the thermocline within the newly developed Texas A&M University high-resolution coupled regional climate model (TAMU_CRCM). We also discuss the role of atmosphere-ocean feedbacks in amplifying the bias.

The atmospheric component of the TAMU_CRCM is the Weather Research and Forecasting model (WRF; Skamarock et al. 2008) Version 3.1.1, which is configured with 27 km horizontal resolution and 28 vertical levels on a domain covering 110°W – 27°E and 46°S – 61°N. The ocean is represented by the Regional Ocean Modeling System (ROMS; http://www.myroms.org/), configured with 9 km horizontal resolution and 30 vertical levels over 98°W – 22°E and 33°S – 52°N. SST, precipitation minus evaporation, surface wind, and latent heat, sensible heat, and radiative fluxes are exchanged every hour. Both models use aligned Arakawa C grids so variables are not interpolated during coupling. Boundary conditions are based on the 0.5° resolution 6-hourly 2001 – 2008 climatology of the National Center for Environmental Prediction Climate Forecast System Reanalysis (NCEP CFSR; Saha et al. 2010), except for SSTs in the uncoupled simulations, which are prescribed from the 0.25° resolution NOAA Optimum Interpolation SST V2 (Reynolds et al. 2007) daily 2001 – 2008 climatology. Initializing the coupled model with the CFSR SST, which is damped to the Reynolds SST, introduces relatively little bias.

Extensive numerical experiments were carried out to test the sensitivity of the model mean climate to physical parameterizations. Here we highlight two uncoupled atmosphere-only and

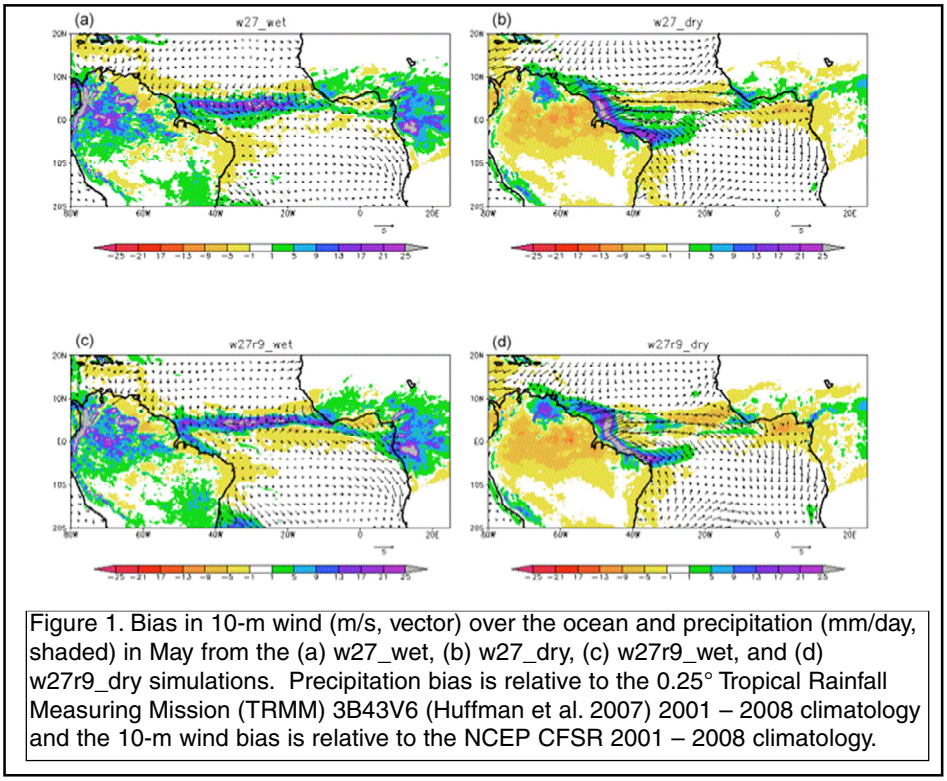

Figure 1. Bias in 10-m wind (m/s, vector) over the ocean and precipitation (mm/day, shaded) in May from the (a) w27_wet, (b) w27_dry, (c) w27r9_wet, and (d) w27r9_dry simulations. Precipitation bias is relative to the 0.25° Tropical Rainfall Measuring Mission (TRMM) 3B43V6 (Huffman et al. 2007) 2001 – 2008 climatology and the 10-m wind bias is relative to the NCEP CFSR 2001 – 2008 climatology.

two coupled atmosphere-ocean experiments (run May 1 – October 1) conducted with atmospheric parameterizations chosen to test the hypothesis that trade wind and precipitation biases drive the summer EEA SST bias. An uncoupled (w27_wet) and a coupled (w27r9_wet) simulation are run with longwave radiation, shortwave radiation, and convection represented by the Rapid Radiative Transfer Model (RRTM), Goddard, and Betts-Miller-Janjic scheme, respectively. An additional uncoupled (w27_dry) and coupled (w27r9_dry) set of simulations is run with the CAM longwave and shortwave radiation and Kain-Fritsch convection. Figure 1 shows the precipitation and 10-m wind bias in the first month of integration. The w27_wet simulation (Fig. 1a) produces a wet bias – in some parts over 20 mm/day – over the Amazon and Congo basin with a weak (1 – 2 m/s) westerly trade wind bias in the EEA. The w27_dry experiment (Fig. 1b) simulates a rainfall deficit (over 10 mm/day) over the Amazon with weaker drying over equatorial Africa and an erroneous rainfall band along the northeastern South American coast. There is also a considerable westerly trade wind bias (over 10 m/s) in the western Atlantic basin in w27_dry. These biases in w27r9_dry, as well as major biases in the large-scale circulation throughout the troposphere (not shown) are related to an over-representation of low-level clouds over the Amazon that leads to a cold land-surface temperature bias and descending mid-tropospheric vertical motion. The trade wind and Amazon precipitation biases of w27_dry are similar to those simulated by most uncoupled and coupled GCMs discussed in Richter and Xie (2008). The rainfall and wind biases are similar between the uncoupled and coupled regional model experiments (except for a stronger westerly wind bias of 1 – 2 m/s along the west coast of equatorial Africa in w27r9_wet (Fig. 1c) compared to w27_wet) indicating that, as in many GCMs, the precipitation and trade wind bias in TAMU_CRCM originates in the atmospheric component.

Although the westerly springtime equatorial trade wind bias in w27r9_dry (Fig. 1d) is of a stronger magnitude and spans a greater portion of the Atlantic basin than that of w27r9_wet (Fig. 1c), the warm summer EEA SST bias is more severe in w27r9_wet. The JJA averaged SST and 10-m wind bias of w27r9_wet and w27r9_dry are shown in Figure 2a and b, respectively. In w27r9_wet there is a cold SST bias of 1 – 2°C in the western equatorial Atlantic and a warm bias of 4 – 5°C concentrat-

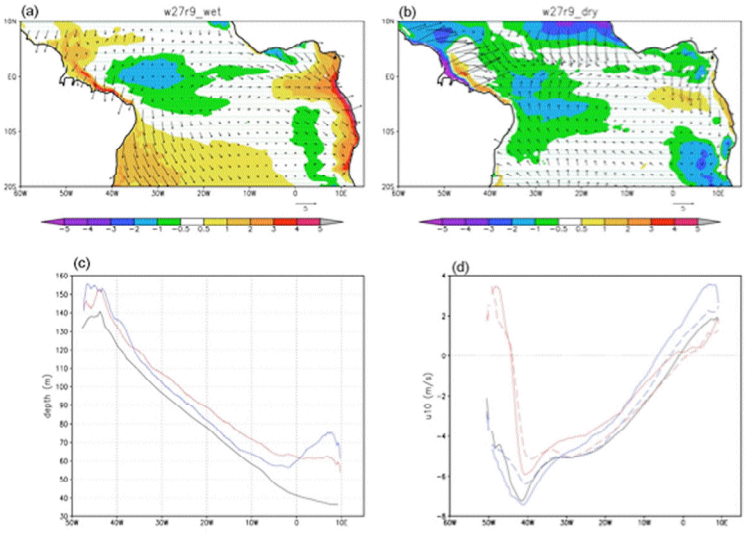

Figure 2. Bias in SST (°C, shaded) relative to the 2001 – 2008 Reynolds climatology and 10-m wind (m/s, vector) over the ocean relative to the NCEP CFSR 2001 – 2008 climatology during JJA from the (a) w27r9_wet and (b) w27r9_dry simulations. (c) Thermocline (20° isotherm) depth (m) during JJA averaged 2°S – 2°N from the NCEP CFSR 2001 – 2008 climatology (black), w27r9_wet (blue), and w27r9_dry (red). (d) The zonal wind at 10-m (m/s) over the ocean during JJA averaged 2°S – 2°N from the NCEP CFSR 2001 – 2008 climatology (black), w27r9_wet (solid blue), w27r9_dry (solid red), w27_wet (dash blue), and w27_dry (dash red).

ed along the west coast of equatorial Africa that extends west to 5°W and decreases to 2 – 3°C. The warm bias also extends into the SETA. The tropical Atlantic SST bias in w27r9_wet resembles that of typical AOGCMs, suggesting that simply increasing model resolution is unlikely to solve this bias problem. Over the EEA there is a westerly surface wind bias of 2 – 3 m/s that is strongest along the coast. The EEA warm SST bias peaks in July at up to 5°C along the coast, while the SETA bias becomes progressively worse throughout the integration (not shown). The warm bias in both regions is confined to the coast during the initial development and spreads west in the following months. The w27r9_dry simulation (Fig. 2b) produces a cool SST bias in the western equatorial Atlantic similar to that of w27r9_wet, but unlike w27r9_wet simulates a weak bias (+/- 1°C) in the EEA and a cold bias in the SETA. The westerly wind bias in the western Atlantic persists into the summer in w27r9_dry. This simulation also exhibits a weak easterly bias in the EEA and a strong northerly wind bias between the equator and 10°N associated with a southward displacement of the ITCZ. The stronger warm EEA SST bias in w27r9_wet suggests that in this regional coupled model the bias is more sensitive to the local rather than basin-wide equatorial trade wind bias, and to excessive rainfall in the Congo basin rather than deficient Amazon rainfall.

The response of the thermocline, represented as the 20°C isotherm depth, supports the idea that the EEA SST bias is more sensitive to local trade winds. Figure 2c shows the thermocline averaged from 2°S – 2°N in JJA from the CFSR reanalysis and the two coupled simulations. There is a steep zonal gradient in the reanalyzed thermocline, which is deep in the west and shallow in the east. To the west of 10°W, w27r9_wet and w27r9_dry simulate a relatively small (5 – 10 m) thermocline bias, whereas to the east w27r9_dry (w27r9_wet) produces a thermocline that is too deep by 20 m (over 30 m). In w27r9_wet, the bias in thermocline depth is so large that the zonal gradient is incorrect. The easterly wind bias in the EEA in w27r9_dry may partly counteract the thermocline bias driven by the almost basin-wide westerly bias. While the basin-wide wind bias in w27r9_dry does induce a thermocline bias in the EEA, it is not as severe as the bias driven by the local winds in w27r9_wet (Fig. 1c and 2a).

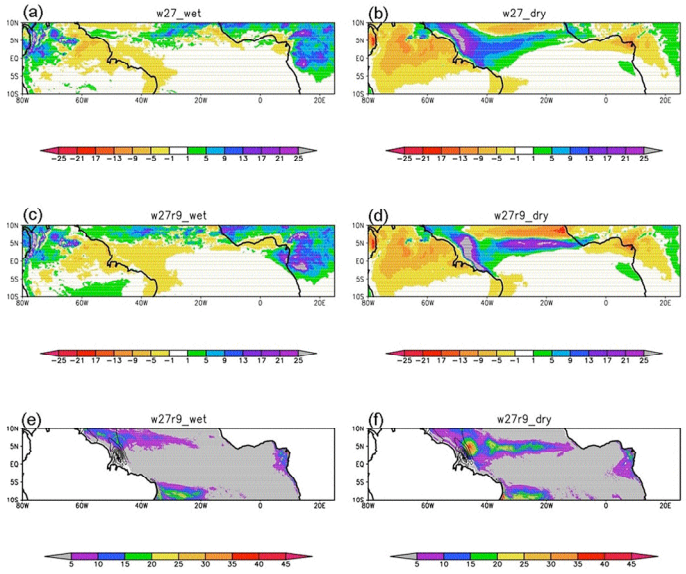

Figure 3. Bias in precipitation (mm/day, shaded) in JJA relative to the TRMM 2001 – 2008 climatology from the (a) w27_wet, (b) w27_dry, (c) w27r9_wet, and (d) w27r9_dry simulations. Barrier layer thickness (m, computed as in Breugem et al. 2008) in JJA from (e and f) the CFSR 2001 – 2008 climatology (contoured every 10 m) and (e) w27r9_wet (shaded) and (f) w27r9_dry (shaded).

The SST and thermocline response in w27r9_wet, together with the difference in the 10-m zonal wind bias between w27r9_wet and w27_wet, suggest that the Bjerknes feedback is important on a local scale in supporting the EEA SST bias. Figure 2d shows the 10-m zonal wind averaged 2°S – 2°N during JJA from the CFSR reanalysis and the coupled and uncoupled simulations. In both the "wet" and "dry" experiments, the trade wind bias is amplified by coupling, similar to typical AGCM and AOGCM simulations. In the EEA there is a slight (less than 1 m/s) westerly bias in w27_wet, that is amplified (over 2 m/s) and strongest along the west coast of Africa in the corresponding coupled simulation. In the "dry" case, the coupling worsens the westerly wind bias in the center of the Atlantic rather than EEA.

Figure 3a – d shows the precipitation bias for the uncoupled and coupled simulations in JJA. The w27_dry (Fig. 3b) and w27r9_dry (Fig. 3d) simulations both produce a dry bias (over 10 mm/day) over the Amazon, a weaker dry bias over equatorial Africa, and – similar to many GCMs – a southward shift of the ITCZ that is amplified in the coupled simulation. In both w27_wet (Fig. 3a) and w27r9_wet (Fig. 3c), the latitudinal position of the ITCZ resembles the observed, but rainfall rates are too high. There is also a wet (dry) bias over the western (eastern) Amazon and a strong wet bias of up to 20 mm/day over equatorial Africa. In w27r9_wet there is also a wet precipitation bias of over 20 mm/day concurrent with the warm EEA SST bias that does not exist in the corresponding uncoupled simulation. This would suggest a rainfall – BL – SST feedback. However, erroneous BLs are simulated in both w27r9_wet (Fig. 3e) and w27r9_dry (Fig. 3f), indicating that the role of barrier layers may be secondary to the wind-driven bias. Coupled simulations with corrected precipitation minus evaporation flux are planned to better understand this problem.

Acknowledgements

This work is supported by DOE grant # DE-SC0004966 and by NOAA grant # NA09OAR4310135. Simulations were run at the Texas A&M Supercomputing Facility. The authors

thank Howard Seidel for his initial contribution to the development of TAMU_CRCM.

References

Balaguru, K., P. Chang, R. Saravanan, and C. J. Jang, 2011: The Barrier Layer of the Atlantic warmpool: Formation mechanism and influence on the mean climate. Tellus (submitted).

Biasutti, M., A. H. Sobel, and Y. Kushnir, 2006: AGCM Precipitation biases in the tropical Atlantic. J. Climate, 19, 935 – 925.

Bjerknes, J., 1969: Atmospheric teleconnections from the Equatorial Pacific. Monthly Weather Review, 97, 163 – 172.

Breugem, W. –P., W. Hazeleger, and R. J. Haarsma, 2006: Multimodel study of tropical Atlantic variability and change. Geophy. Res. Lett., 33, doi: 10.1029/2006GL027831.

Breugem, W. –P., P. Chang, C. J. Jang, J. Mignot, and W. Hazeleger, 2008: Barrier layers and tropical Atlantic SST biases in coupled GCMs. Tellus, 60A, 885 – 897.

Chang, C. -Y., J. A. Carton, S. A. Grodsky, and S. Nigam, 2007: Seasonal climate of the tropical Atlantic sector in the NCAR Community Climate System Model 3: Error structure and probable causes of crrors. J. Climate, 20, 1053 – 1070.

Chang, C. -Y., S. Nigam, and J. A. Carton, 2008: Origin of the springtime westerly bias in Equatorial Atlantic surface winds in the Community Atmosphere Model Version 3 (CAM3) simulation. J. Climate, 21, 4766 – 4778.

Davey, K. M., and Coauthors, 2002: STOIC: A study of coupled model climatology and variability in tropical ocean regions. Clim. Dyn., 18, 403 – 420.

DeWitt, D. G., 2005: Diagnosis of the tropical Atlantic near-equatorial SST bias in a directly coupled atmosphere-ocean general circulation model. Geophys. Res. Lett., 32, doi:10.1029/2004GL021707.

Hazeleger, W., and R. J. Harrsma, 2005: Sensitivity of tropical Atlantic climate to mixing in a coupled ocean–atmosphere model. Clim. Dyn., 25, 387 – 399.

Huang, B., Z. –Z. Hu, and B. Jha, 2007: Evolution of model systematic errors in the tropical Atlantic basin from coupled climate hindcasts. Clim. Dyn., 28, 661 – 682.

Huffman, G.J., R.F. Adler, D.T. Bolvin, G. Gu, E.J. Nelkin, K.P. Bowman, Y. Hong, E.F. Stocker, D.B. Wolff, 2007: The TRMM multi-satellite precipitation analysis: Quasi-global, multi-year, combined-sensor precipitation estimates at fine scale. J. Hydrometeor., 8, 38-55.

Lamb. P. J., 1978: Case studies of tropical Atlantic surface circulation patterns during recent sub-Saharan weather anomalies: 1967 and 1968. Monthly Weather Review, 106, 482 – 491.

Large, W. G., and G. Danabasoglu, 2006: Attribution and impacts of upper-ocean biases in CCSM3. J. Climate, 19, 2325 – 2346.

Mitchell, T.P. and J.M. Wallace, 1992: The annual cycle in equatorial convection and sea surface temperature, J. Climate, 5, 1140-1156.

Philander, S. G. H., and R. C. Pacanoswki, 1981: The oceanic response to cross-equatorial winds (with application to coastal upwelling in low latitudes). Tellus, 33, 201 – 210.

Reynolds, R. W., T. M. Smith, C. Liu, D. B. Chelton, K. S. Casey, and M. G. Schlax, 2007: Daily high-resolution-blended analyses for sea surface temperature. J. Climate, 20, 5473 – 5496.

Richter, I., and S. –P. Xie, 2008: On the origin of equatorial Atlantic biases in coupled general circulation models. Clim. Dyn., 31, 587 – 598.

Richter, I., S. –P. Xie, A. T. Wittenberg, and Y. Masumoto, 2011: Tropical Atlantic biases and their relation to surface wind stress and terrestrial precipitation. Clim. Dyn., doi:10.1007/s00382-011-1038-9.

Saha, S., and Coauthors, 2010: The NCEP Climate Forecast System Reanalysis. Bull. Amer. Met. Soc., 1015 – 1057.

Skamarock, W. C., and Coauthors, 2008: A description of the Advanced Research WRF Version 3. NCAR Tech. Note, NCAR/TN-475+STR, 113 pp.

Vizy, E. K., and K. H. Cook, 2002: Development and application of a mesoscale climate model for the tropics: Influence of sea surface temperature anomalies on the West African monsoon. J. Geophys. Res., 107, doi: 10.1029/2001JD000686.

Wahl, S., M. Latif, W. Park, and N. Keenlyside, 2001: On the tropical Atlantic SST warm bias in the Kiel Climate Model. Clim. Dyn., 36, 891 – 906.

Ward, N. M., 1998: Diagnosis and short-lead time prediction of summer rainfall in tropical North Africa at interannual and multidecadal timescales. J. Climate, 11, 3167 – 3191.

Xu, Z., M. Li, P. Chang, and R. Saravanan, 2011: Oceanic origin of tropical Atlantic biases (in preparation).

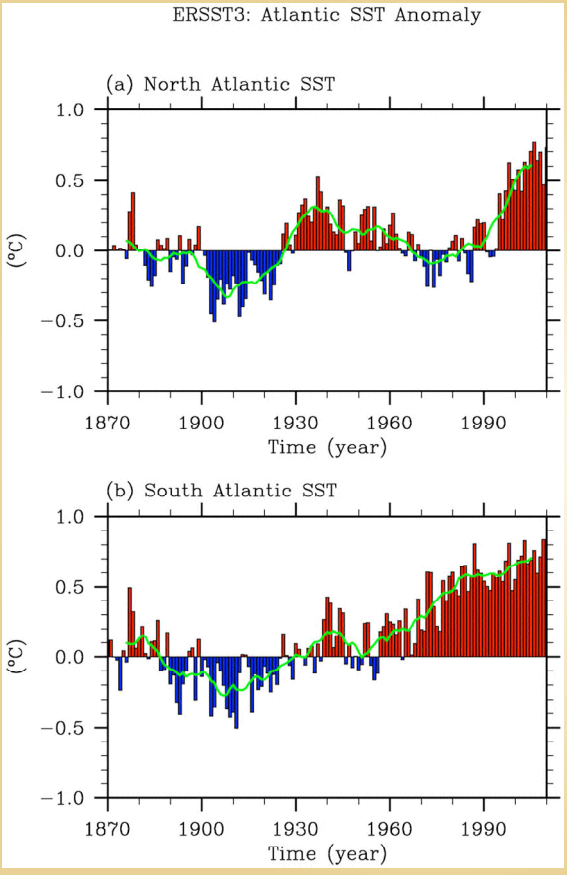

Figure1. Observed (a) North (0^O – 60^ON) and (b) South Atlantic (30^OS – 0^O) SSTs during the instrumental period, obtained from ERSST3. The green line in each plot is obtained by performing a 11-year running average.

Figure associated with article on the following page

Secular and Multidecadal Warming of the Atlantic Ocean since the mid-20th Century

Sang-Ki Lee[1,2], David B. Enfield[1,2], Wonsun Park[3], Erik van Sebille[5], Chunzai Wang[2], Steven Yeager[4], Ben Kirtman[5], and Molly Baringer[2]

[1]Cooperative Institute for Marine and Atmospheric Studies, University of Miami, Miami, Florida
[2]Atlantic Oceanographic and Meteorological Laboratory, NOAA, Miami, Florida
[3]Leibniz Institute of Marine Sciences (IFM-GEOMAR), Kiel, Germany
[4]National Center for Atmospheric Research, Boulder, Colorado
[5]Rosenstiel School for Marine and Atmospheric Science, University of Miami, Miami, Florida

As seen in the extended reconstructed sea surface temperature data (ERSST3; Smith et al., 2008), the North Atlantic sea surface temperature (SST) during the instrumental period (Figure 1a) contains both a secular increase at a rate of ~ 0.4^{o}C per 100yrs during 1901-2010 and a robust multidecadal signal of similar amplitude, known as the Atlantic multidecadal oscillation (AMO; Kerr, 2000). Coupled general circulation models forced by external factors such as greenhouse gases and solar variations do a poor job of reproducing the AMO in the 20th century, suggesting that it must arise instead from internal interactions of the climate system (e.g., Knight, 2009). It has been shown that in an unforced coupled climate model simulation the Atlantic meridional overturning circulation (AMOC) exhibits decadal to multidecadal (15 - 70 yrs) variations and is closely linked both dynamically and statistically to the AMO (e.g., Delworth et al., 1993). However, neither the long-term variations of the AMOC nor the link between the AMOC and AMO has been demonstrated with observations in the 20th century because historical observations of the AMOC are not up to the task.

Contrary to the North Atlantic SST, the South Atlantic SST during the instrumental period (Figure 1b - shown left) has increased almost linearly at a rate of ~ 0.9^{o}C per 100yrs during 1901-2010, clearly surpassing the global average of 0.6 ~ 0.7^{o}C per 100 yrs. Consistent with this surface trend, recently updated and bias-corrected instrumental records indicate that the heat content of the Atlantic Ocean in the upper 700m has substantially increased during the 1970s – 2000s at a rate (~ 8x10^{22} J per 40yrs) almost matching that of the Pacific Ocean (~ 6x10^{22} J per 40yrs) and Indian Ocean (~ 2x10^{22} J per 40yrs) combined (Levitus et al., 2009), even though the Atlantic Ocean covers less than 20% of the global ocean in surface area. As a candidate mechanism for the differential inter-ocean warming, Lee et al. (2011) pointed out the potential role played by the global overturning circulation. They argued that as the upper ocean warms globally during the 20th century, the inter-ocean heat transport associated with the global overturning circulation should increase until the deep ocean fully adjusts to the surface warming or the global overturning circulation slows down. Since the Atlantic Ocean is characterized with advective heat convergence, they argued that the Atlantic Ocean should therefore gain extra heat from other oceans. They used a surface-forced global ocean-ice coupled model to test this hypothesis and to further show that the increased AMOC at 30^{o}S, forced by the increased wind stress curl over the region from 50^{o} to 30^{o}S, has contributed greatly to the increased inter-ocean heat transport from the Indian Ocean during the latter half of the 20th century.

To sum up, it appears that the AMOC and the associated meridional ocean heat transport hold the key to our understanding of the observed secular and multidecadal warming of the North and South Atlantic Oceans since the mid-20th century. Therefore, it is vital to reconstruct the history of AMOC and associated meridional ocean heat transport in the 20th century, covering at least one full cycle of the AMO to be able to cleanly distinguish the secular trend from the multidecadal variations. Here, we attempt an ocean model-based reconstruction, which is likely to be our best chance for assessing the history of AMOC in the 20th century because the observed surface flux fields, which constrain ocean-only (or ocean-ice coupled) models, are available on relatively long time scales.

20th Century Reanalysis (20CR)

None of the surface-forced ocean model studies so far has been simulated with the surface forcing prior to the mid-20th century because the surface forcing data, which are typically derived from atmospheric reanalysis products such as NCEP-NCAR reanalysis, are limited to the last 50 - 60 years. Recently, the newly developed NOAA-CIRES 20th Century Reanalysis (20CR) has been completed (Compo et al., 2010). The 20CR provides the first estimate of global surface momentum, heat and freshwater fluxes spanning the late 19th century and the entire 20th century (1871-2008) at daily temporal and 2^{o} spatial resolutions.

Model Experiments

The global ocean-ice coupled model of the NCAR Community Climate System Model version 3 (CCSM3) forced with the 20CR is used as the primary tool in this study. The ocean model is a level-coordinate model based on the Parallel Ocean Program (POP),

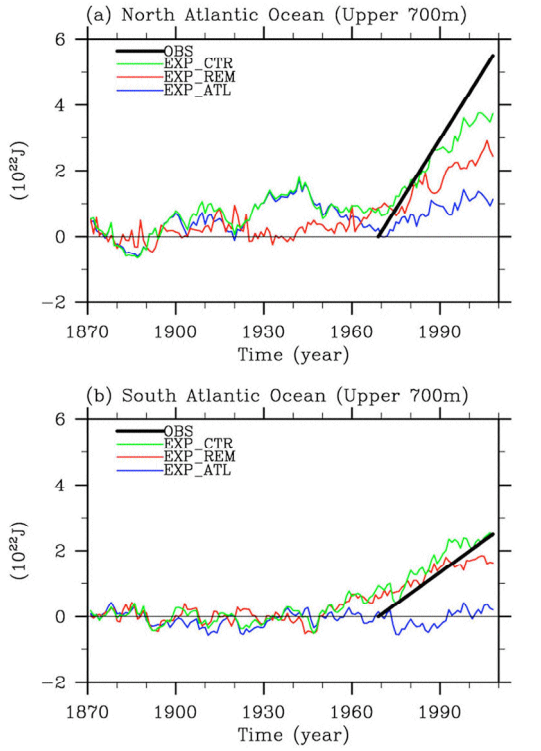

Figure 2. Simulated (a) North and (b) South Atlantic Ocean heat content changes in the upper 700m in reference to 1871-1900 obtained from the three model experiments. The thick black lines in (a) and (b) are the observed trends of the North and South Atlantic Ocean heat content, respectively, reproduced from Levitus et al. (2009).

divided into 40 vertical levels. The ice model, the NCAR Community Sea Ice Model version 5, is a dynamic-thermodynamic ice model. Both the ocean and ice models have 320 longitudes and 384 latitudes on a displaced pole grid with a longitudinal resolution of about 1.0 degrees and a variable latitudinal resolution of approximately 0.3 degrees near the equator. See Doney et al. (2007) for more detailed descriptions about the CCSM3 ocean-ice model (CCSM3_POP hereafter).

After the total of 900 years of spin up runs (see Lee et al. (2011) for a detailed description of the spin up runs), three model experiments are performed. In the control experiment (EXP_CTR), the CCSM3_POP is integrated for 1871-2008 using the real-time daily 20CR surface flux fields. The next two experiments are idealized experiments designed to understand the Atlantic Ocean heat content change with and without the influence of the northward heat transport change at 30^{o}S. The remote ocean warming experiment (EXP_REM) is identical to EXP_CTR except that the surface forcing fields north of 30^{o}S are from the daily 20CR surface flux fields for the period of 1871-1900 exactly like the spin-up experiment, whereas those south of 30^{o}S are real time as in EXP_CTR. The Atlantic Ocean warming experiment (EXP_ATL) is also identical to EXP_CTR except that the surface forcing fields south of 30^{o}S are from the daily 20CR surface flux fields for the period of 1871-1900 as in the spin-up experiment, whereas those north of 30^{o}S are real time as in EXP_CTR. Note that the Atlantic Ocean warms only through anomalous surface warming (i.e., local processes) in EXP_ATL, and only through anomalous northward ocean heat transport at 30^{o}S (i.e., remote processes) in EXP_REM, respectively.

Model Results

Figure 2a shows the simulated North Atlantic Ocean heat content change in the upper 700m in reference to the 1871 - 1900 period obtained from the three model experiments, along with the observed trend of the North Atlantic Ocean heat content during 1969 – 2008. The observed trend is referenced at 1969 in Figure 2 for a better visual comparison with the simulated trends. The simulated North Atlantic Ocean heat content in EXP_CTR increases moderately during the 1930s - 1940s, and then decreases during the 1940s - 1970s, after which it increases substantially much like the AMO from observations (Figure 1a). Between the 1970s and 2000s, it increases by 3 ~ 4x10^{22} J. This large increase is reasonably close to the observed North Atlantic Ocean heat content increase of ~ 5.5x10^{22} J during the same period (Levitus et al., 2009), suggesting that the model experiment (EXP_CTR) reproduces reasonably well the heat budget trend of the North Atlantic Ocean after the 1960s.

If the northward heat transport in the South Atlantic at 30^{o}S is fixed at its 1871-1900 level by considering the fully transient surface fluxes only north of 30^{o}S (EXP_ATL), the simulated North Atlantic Ocean heat content increases during the 1930s - 1940s, and then decreases during the 1940s - 1970s, almost perfectly reproducing that of EXP_CTR prior to the 1970s. However, the North Atlantic Ocean heat content, in this case, increases by only ~ 1x10^{22} J during the 1970s and 2000s, and thus cannot explain the observed North Atlantic Ocean heat content increase during the same period.

On the other hand, if the northward heat transport in the South Atlantic at 30^{o}S is allowed to vary in real time by considering the fully transient surface fluxes south of 30^{o}S while keeping the surface fluxes over the Atlantic Ocean at their 1871-1900 levels (EXP_REM), the North Atlantic Ocean heat content increases by ~ 2 x10^{22} J during the 1970s – 2000s explaining a moderate portion of the observed trend. In this case, however, the multidecadal signal during the 1930s – 1970s, which is clearly simulated in both EXP_CTR and EXP_ATL is completely missing. The absence of this multidecadal signal in EXP_REM and its presence in EXP_ATL clearly suggest that the multidecadal swing in EXP_CTR prior to the 1970s is caused by processes internal to the Atlantic Ocean. During the 1970s – 2000s, on the other hand, remote processes (i.e., increased inter-ocean heat transport from the Indian Ocean; see Lee et al. (2011)) have contributed more to the large increase in the North Atlantic heat content, although internal processes have also contributed.

Figure 2b is the same as Figure 2a, except for the South Atlantic Ocean heat content change. The simulated South Atlantic Ocean heat content in EXP_CTR remains unchanged until the

1960s, after which it increases monotonically, consistent with the similar increase in the South Atlantic SST during the same period from observations (Figure 1b). Between the 1970s and 2000s, it increases by ~ 2 x10^{22} J, slightly less than the observed South Atlantic Ocean heat content increase of ~ 2.5x10^{22} J during the same period (Levitus et al., 2009). As in EXP_CTR, the South Atlantic Ocean heat content in EXP_REM is also characterized with a monotonic increase after the 1960s, but with a smaller amplitude of 1~ 2x10^{22} J during the 1970s – 2000s. In the case of EXP_ATL, however, there is no apparent change in the South Atlantic heat content throughout the 20th century. These results derived from Figure 2b lead to a conclusion that remote processes mainly drive the South Atlantic Ocean heat content increase during the 1970s - 2000s in EXP_CTR.

Figure 3a shows the time-averaged AMOC during 1979-2008 obtained from EXP_CTR. The simulated maximum strength of the AMOC at 35^{o}N is only 11 Sv (1Sv = 106 m^3s^{-1}), which is smaller than the observed range of 14 ~ 20Sv. Despite the smaller maximum strength, the overall spatial structure of the simulated AMOC is quite close to that derived from observations (e.g., Lumpkin and Spear, 2007). Figure 3b shows the time series of the simulated AMOC index (maximum overturning stream function) at three different latitudes, namely 30^{o}S, the equator, and 60^{o}N, in reference to the 1871 – 1900 period. It is clear that the AMOC at all three latitudes increase after the 1950s, with the largest amplitude at 30^{o}S, a lesser amplitude at the equator, and the smallest amplitude at 60^{o}N. This suggests that both the North (0^{o} – 60^{o}N) and South (30^{o}S – 0^{o}) Atlantic Oceans are subject to advective heat convergence during the 1960s – 2000s, consistent with the heat content increase in the North and South Atlantic Oceans during the 1970s – 2000s (Figure 2).

Additional work is needed to understand how the AMOC is linked with the multidecadal variations of the North Atlantic Ocean heat content prior to the 1960s.

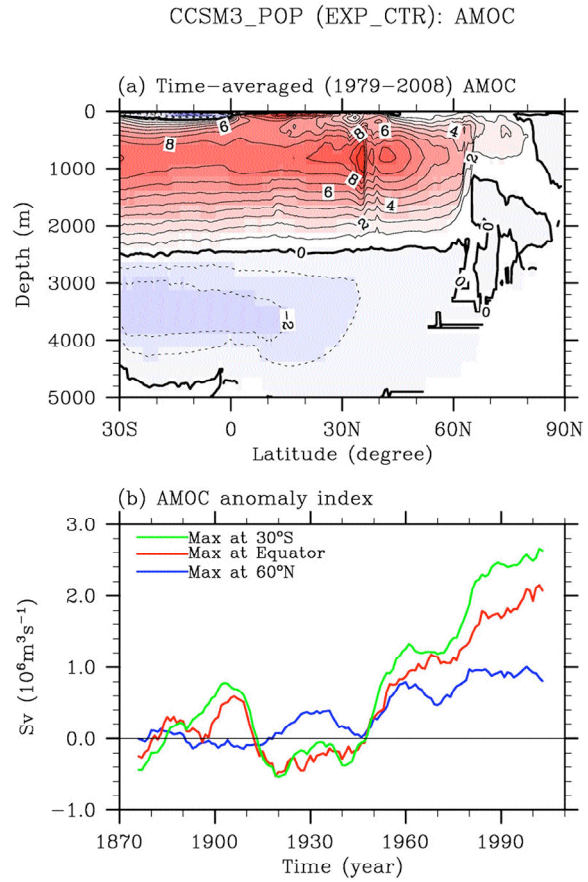

Figure 3. (a) Time-averaged AMOC during 1979-2008 and (b) 11-year running averaged time series of the simulated AMOC index (maximum overturning stream function) at 30^{o}S, the equator, and 60^{o}N in reference to 1871-1900 obtained from EXP_CTR.

Acknowledgments

This study was motivated and benefited from the AMOC discussion group of the research community at UM/RSMAS and NOAA/AOML. We wish to thank Igor Kamenkovich and all the participants who led the AMOC discussion group during the past year. We acknowledge helpful suggestions from Ping Chang. This work was supported by grants from the National Oceanic and Atmospheric Administration's Climate Program Office and by grants from the National Science Foundation.

References

Compo, G. P., and collaborators, 2011: The twentieth century reanalysis project. Quarterly J. Roy. Meteorol. Soc., 137, 1-28. doi: 10.1002/qj.776.

Delworth, T., S. Manabe, and R. Stouffer, 1993: Interdecadal variations of the thermohaline circulation in a coupled ocean-atmosphere model. J. Climate, 6, 1993–201.

Doney, S. C., Steve Yeager, G. Danabasoglu, W. G. Large, and J. C. McWilliams, 2007: Mechanisms governing interannual variability of upper-ocean temperature in a global ocean hindcast simulation. J. Phys. Oceanogr., 37, 1918–1938.

Kerr, R. A., 2000: A North Atlantic climate pacemaker for the centuries. Science, 288, 1984-1986.

doi:10.1126/science.288.5473.1984.

Knight, Jeff R., 2009: The Atlantic multidecadal oscillation inferred from the forced climate response in coupled general circulation models. J. Climate, 22, 1610–1625.

Lee S.-K., W. Park, E. van Sebille, C. Wang, D. B. Enfield, S. Yeager, B. P. Kirtman, and M. O. Baringer, 2011: What caused the significant increase in Atlantic ocean heat content since the mid-20th century? Geophys. Res. Lett. (submitted).

Levitus, S., J. I. Antonov, T. P. Boyer, R. A. Locarnini, H. E. Garcia, and A. V. Mishonov, 2009: Global ocean heat content 1955–2008 in light of recently revealed instrumentation problems. Geophys. Res. Lett., 36, L07608. doi:10.1029/2008GL037155.

Lumpkin, R. and K. Speer, 2007: Global ocean meridional overturning. J. Phys. Oceanogr., 37, 2550-2562.

Workshop on Coupled Ocean-Atmosphere-Land Processes in the Tropical Atlantic

Paquita Zuidema, C. Roberto Mechoso, and Laurent Terray

Coupled GCMs suffer from common biases in the Pacific and Atlantic basins. While the newer-generation CCSM4 has demonstrated an overall reduced SST bias compared to CCSM3, it nevertheless retains a similar SST-bias spatial pattern (Gent et al., 2010). Significantly, however, model improvements have had less impact on the simulated SSTs in the Atlantic than for the Pacific. The Atlantic still exhibits the most severe bias problem among all the tropical oceans in the current generation of climate models. In fact, the Atlantic bias problem is still so severe that some of the most fundamental features of the equatorial Atlantic Ocean – the east-west equatorial SST gradient and the eastward shoaling thermocline – cannot be reproduced by most coupled climate models.

The lack of progress in the Atlantic bias problem may be attributed to two major factors: 1) the complex nature of the bias problem and 2) a lack of focused attention from the research community. Hypotheses for a complex Atlantic bias problem tend to draw on the fundamental observation that the Atlantic basin is far smaller than the Pacific basin. The smaller Atlantic basin compared to the Pacific encourages a tighter and more complex land-atmosphere-ocean interaction with not just the east side of the ocean basin, but also its west side. Hypotheses can be oceanic (e.g., insufficient upwelling in the eastern basin because local processes are not resolved); atmospheric (e.g., poor representation of the winds; cloud decks that are too thin); land-based (e.g., poorly represented deep convection over land; biomass-burning aerosol direct radiative impacts that vary with whether the underlying surface is cloud or ocean) and can be of both local and remote origins (e.g., remote forcings from the Pacific onto the Atlantic). As already suggested by the examples given here, many hypotheses reflect truly coupled processes between ocean, land, and atmosphere. Several of these are detailed further here in other articles.

In March 23-24, 2011, a workshop was held at the University of Miami to specifically focus on the bias problem in the tropical Atlantic. A goal of the workshop was to bring together disparate communities working on research relevant to the hypotheses for the model biases, and to identify a network of interested researchers. The workshop received support from both US funding agencies and from WCRP. Participation in the workshop was international and at a high level of expertise. Approximately 85 people participated; the agenda and all the presentations are available through http://www.clivar.org/organization/atlantic/meetings/tropical_bias/miami.php. Interest in this problem is clearly high.

A major workshop objective was to develop a coherent synthesis of the state-of-the-art knowledge on the Atlantic SST model biases and their causes for the southeast and eastern tropical Atlantic, as well as a set of sharpened hypotheses. This is an ambitious goal, and although many ideas were put forth, the 2.5 days were not enough to form a consensus view, or even to integrate all the information. The workshop confirmed many hypotheses, but did not rank them. The workshop also revealed that while there are efforts underway to address the hypotheses using models, the interaction with observational programs is still weak. Observational programs have collected data, but they are still in the synthesis stage. Further work still needs to be done to articulate an effective way forward (further model analysis? new coordinated model experiments? new field programs, or modification of existing observational networks?), and to define an appropriate geographical focus.

At the time of this writing, the next steps forward are being discussed, and are expected to lead to both formal and informal task teams aimed at further articulating, ranking, and addressing approaches to causes for the coupled model SST biases. These will lead to a report highlighting similarities and differences between GCM performance in the tropical Atlantic and Pacific; a written survey of field programs completed, in progress, or under development; better definition of an appropriate geographical foci; development of diagnostics and metrics for model validation; and promotion of international collaborations between observational and modeling studies. These efforts will help refine the ultimate goal: to articulate the best way to reduce coupled model SST biases using targeted process studies and model assessments.

U.S. CLIVAR
Climate Variability & Predictability

U.S. CLIVAR OFFICE
1717 Pennsylvania Avenue, NW
Suite 250
Washington, DC 20006

Subscription requests, and changes of address should be sent to the attention of the U.S. CLIVAR Office (cstephens@usclivar.org)

WCRP
World Climate Research Programme

U.S. CLIVAR contributes to the CLIVAR Program and is a member of the World Climate Research Programme

This material was developed with federal support of NASA, NOAA and NSF through the NSF Cooperative Agreement No. AGS-0926904. Any opinions, findings, conclusions or recommendations expressed in this material are those of the author(s) and do not necessarily reflect the views of the sponsoring agencies.

Climate Variability & Predictability
CLIVAR
World Climate Research Programme